A simulation on the global mean structure of the ionosphere and thermosphere

Z. Ren[1], W. Wan[1], L. Liu[1]

[1]Institute of Geology and Geophysics, Chinese Academy of Sciences. **Address**: No. 19, Beitucheng Western Road, Chaoyang District, 100029, Beijing, P.R.China. **Email**: zpren@mail.iggcas.ac.cn

Abstract

In this paper, we examine the global mean structures of the ionosphere and thermosphere for geomagnetic quiet condition using a new global three-dimensional self-consistent model of the ionosphere and thermosphere (GCITEM-IGGCAS, Global Coupled Ionosphere-Thermosphere-Electrodynamics Model, Institute of Geology and Geophysics, Chinese Academy of Sciences). GCITEM-IGGCAS self-consistently calculates the time-dependent three-dimensional structures of the main parameters of the ionosphere and thermosphere for the height range from 90 to 600 km. For example, neutral number density of O_2, N_2, O, $N(^2D)$, $N(^4S)$, NO, He and Ar; ion number densities of O^+ ,O_2^+, N_2^+, NO^+, N^+ and electron; neutral, electron and ion temperature; neutral wind; and ionospheric electric fields. We simulates the main features of the global mean structures of the ionosphere and thermosphere using this model, and the simulated results agree well with the empirical models. We also simulate the seasonal variations of the global mean structures of the ionosphere and thermosphere in this paper.

1. Introduction

The ionospheric and thermospheric simulations play an important role in the coupled ionosphere-thermosphere system research. A series of ionosphere/thermosphere numerical model had been developed in previous researches. However, the development of global numerical models of the thermosphere and numerical models of the ionosphere have proceeded generally independently of each other, and the background atmospheric and ionospheric properties of these numerical models have usually been obtained from global empirical models of the ionosphere and global empirical models of the thermosphere, such as Mass Spectrometer Incoherent Scatter model (MSIS) [Hedin, 1991] and International Reference Ionosphere (IRI) [Bilitza, 2001].

In order to simulate the complex coupled mechanism between the neutrals and ions, the researches need coupled models of the ionosphere-thermosphere system. To simulate the complex coupled ionosphere-thermosphere system as a whole, a series of global self-consistent models of the thermosphere and ionosphere, such as National Center for Atmospheric Research thermosphere-ionosphere general circulation model (NCAR-TIGCM) [Richmond et al., 1992], Coupled Thermosphere Ionosphere Plasmasphere general circulation model (CTIP) [Fuller-Rowell et al., 1980] and their later variants, have been developed in the last 30 years. With these global coupled self-consistent models, the researchers have simulated studied the neutral and ionized properties of the ionosphere-thermosphere system.

The Global Coupled Ionosphere-Thermosphere-Electrodynamics Model, which is developed at Institute of Geology and Geophysics, Chinese Academy of Sciences (GCITEM-IGGCAS), is a global 3-D self-consistent model of the ionosphere and thermosphere including electrodynamics [Ren et al., 2009]. This model self-consistently calculates the time-dependent 3-D structure of the main parameters of the thermosphere and the ionosphere, including neutral number density of O_2, N_2, O, $N(^2D)$, $N(^4S)$, NO, He and Ar; ion number densities of O^+ ,O_2^+, N_2^+, NO^+, N^+ and electron; neutral, electron and ion temperature; neutral wind fields; and the mid- and low-latitude ionospheric electric fields. It is a full 3-D code with 5° latitude by 7.5° longitude cell for the height range from 90 to 600 km in a spherical geomagnetic coordinate system. This model bases on the hydrostatic assumption, and uses an altitude grid. The vertical grid spacing varies from about 3 km in the lower thermosphere to about 30 km in the upper thermosphere. This model is solved by a time-stepping finite difference procedure, whose time step is 2~5 minutes. The explicit numerical method is used in the horizontal difference procedure, and we use implicit numerical method in the vertical difference procedure. GCITEM-IGGCAS can be used to examine the important

978-1-4673-5225-3/14/$31.00 ©2014 IEEE

aeronomical processes that operate in the atmosphere from 90 to 600 km. In this paper, we use this self-consistent model to examine the global mean structure of the ionosphere and thermosphere for geomagnetic quiet conditions.

2. Global Mean Structures of the Thermosphere and Ionosphere

We simulated the global mean structures of the thermosphere and ionosphere and their seasonal variations. These simulations were performed for geomagnetic quiet conditions, corresponding to a cross cap potential of 20 kV and auroral particle precipitation with a hemispheric power of 10 GW. Most of these simulations were performed for media solar flux level, corresponding to a solar 10.7 cm flux index ($F_{10.7}$) of 140 and an 81-day average value of $F_{10.7}$ of 140. The neutral temperature and composition at the low boundary were obtained from MSIS00 empirical model. However, the diurnal and semi-diurnal tide of MSIS00 empirical model are removed, and the diurnal and semi-diurnal tide from Global Scale Wave Model (GSWM00) [Hagan et al., 2001] are added into the low boundary. These simulations were all performed based on an International Geomagnetic Reference Field (IGRF). To examine our results, we also compared our runs with the results from MSIS00 and IRI2000 empirical model.

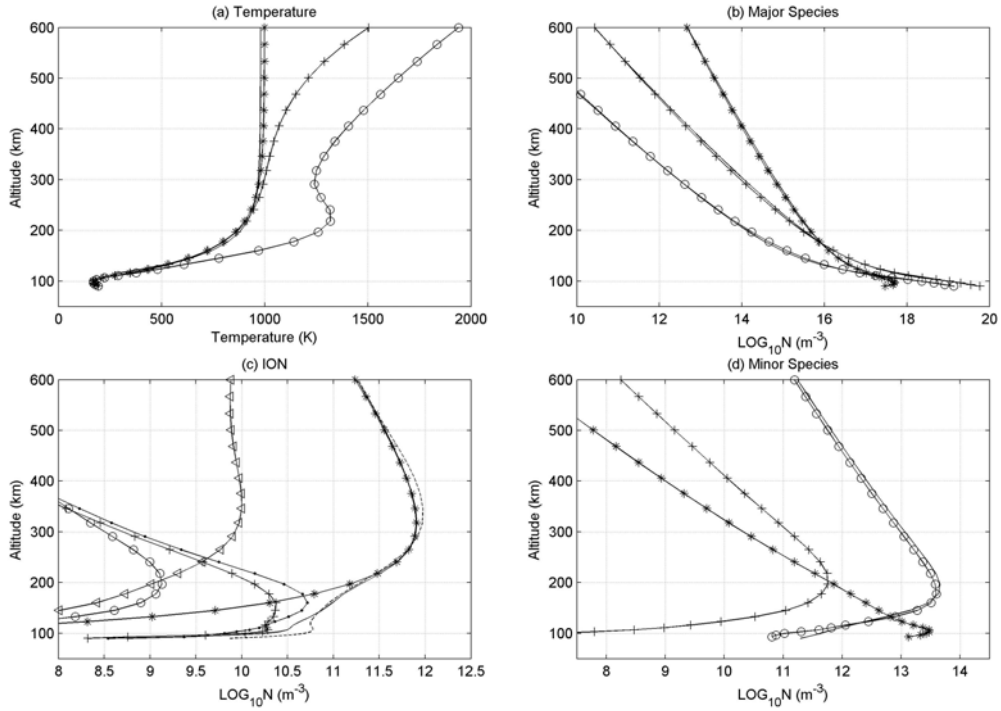

Figure 1. The global mean profiles of the thermospheric and ionospheric parameters for March Equinox. Figure 2a shows that of neutral (star line), ion (plus line) and electron (circle line) temperature (K) from calculation and neutral temperature (solid line) from MSIS00 empirical model. Figure 2b shows that of $\log_{10}$ O (star line), N_2 (plus line) and O_2 (circle line) number densities (m^{-3}) from calculation and from MSIS00 (solid line). Figure 2c shows that of $\log_{10} e$ (solid line), O^+(star line), O_2^+(plus line), NO^+(dot line), N^+(triangle line) and N_2^+(circle line) number densities (m^{-3}) from calculation and $\log_{10} e$ (dashed line) from IRI2000. Figure 2d shows that of $\log_{10}$ NO(star line), N(^{2}D)(plus line) and N(^{4}S)(circle line) number densities (m^{-3}) from calculation and $\log_{10}$ N (solid line) from MSIS00.

Figure 1 shows the global mean profiles of thermosphere and ionosphere. Figure 1a shows the global mean profiles of neutral (star line), ion (plus line) and electron (circle line) temperature from calculation and neutral (solid line) temperature from MSIS00 empirical model in units of K. The maximum calculated global mean neutral temperature is 999K at exospheric heights, and is about 19K higher than MSIS00 result. The minimum calculated global mean neutral temperature is 169 K near the height of 100 km, and is about 10 K lower than MSIS00 result. This result is similar with the result from early simulations and the MSIS00 empirical model. The calculated electron temperature profile is typical of profiles measured and calculated at mid-latitudes, with a

peak temperature near 200 km maintained by strong photoelectron heating. The gradient in electron temperature in the upper thermosphere is maintained by the downward heat flux from the magnetosphere. In the lower thermosphere the ion temperature is nearly equal to the neutral temperature, but at higher altitudes it exceeds the neutral temperature because of electron-ion Coulomb interactions. Figure 1b shows the global mean profiles of O (star line), N_2 (plus line) and O_2 (circle line) number densities from calculation and from MSIS00 (solid line) in units of m^{-3}. The profiles from calculation and from MSIS00 agree throughout. The O number densities from calculation and from MSIS00 both reach their peaks near the height of 97km.

Figure 1c shows the global mean profiles of electron (solid line), O^+(star line), O_2^+(plus line), NO^+(dashdot line), N^+(triangle line) and N_2^+(circle line) number densities from calculation and electron number densities (dashed line) from IRI2000 in units of m^{-3}. The calculated peak electron number density is 8.17×10^{11} m^{-3} at 320km compared to 9.46×10^{11} m^{-3} at 346km predicted by IRI2000. The calculated mean electron density shows similar altitudinal variation with that from IRI2000 model, especially in the lower F region. Molecular ions O_2^+ and NO^+ dominate in the lower thermosphere up to an altitude of about 180 km, and O^+ dominates above. Nitrogen ions N^+ and N_2^+ are minor constituents throughout the ionosphere. Figure 1d shows the global mean profiles of NO (star line), N(^{2}D) (plus line) and N(^{4}S) (circle line) number densities from calculation and N (solid line) from MSIS00 in units of m^{-3}. N(^{2}D) is assumed to be in photochemical equilibrium, with a peak density of 5.70×10^{11} m^{-3} at 200km. The density of N(^{4}S) peaks at 180 km with a value of 3.95×10^{13} m^{-3}, and the NO density peaks near 103km with a value of 2.99×10^{13} m^{-3}. The calculated N(^{4}S) profile agrees well with the globally averaged N density profile from MSIS00 model.

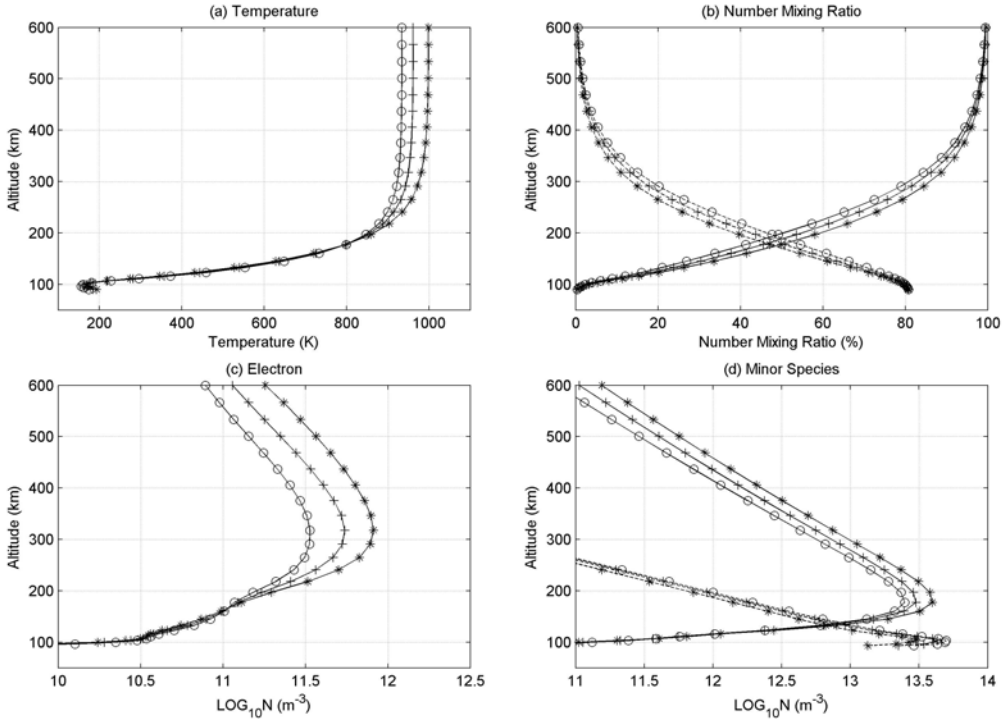

Figure 2. The seasonal variations of the global mean neutral temperature (a), O (solid line in b) and N_2 (dashed line in b) number mixing ratio (%), $\log_{10} e$ (c), NO(dashed line in d) and N(^{4}S)(solid line in d) number densities (m^{-3}) profiles. In all these plots, the star line, plus line and circle line respectively show the altitudinal variations for March Equinox, December solstice, and June solstice.

The thermosphere and ionosphere exhibit significant seasonal variations [Qian et al., 2009; Zeng et al., 2008]. Thus, we also simulate the seasonal variations of the global mean profiles of thermosphere and ionosphere. Figure 2 shows the seasonal variations of global mean neutral temperature (a), O (solid line in b), N_2 (dashed line in b) number mixing ratio (%), $\log_{10} e$ (c), NO(dashed line in d), N(^{4}S)(solid line in d) number densities (m^{-3}) profiles, the circle line, plus line and star line in them respectively show the altitudinal variations for March Equinox, December solstice, and June solstice. Although the profiles for different seasons show similar

altitudinal variations, the obviously seasonal variations can be found. As shown in Figure 2a, although the neutral temperature below 110km do not vary with season obviously, the exospheric temperature show its highest value (999 K) at March Equinox, and its lowest value (934 K) at June solstice. Figure 2b shows that global mean O number mixing ratio show its highest value at March Equinox, and its lowest value at June solstice. The global mean N_2 number mixing ratio shows its lowest value at March Equinox, and its highest value at June solstice. As shown in Figure 2c, although the peak altitudes of the global mean electron number density do not show obvious seasonal variation, the peak values show its highest value (8.17×10^{11} m^{-3}) at March Equinox, and its lowest value (3.38×10^{11} m^{-3}) at June solstice. Figure 2d shows that the peak altitudes of the global mean NO and N(^{4}S) number density do not show obvious seasonal variation. However, the peak values of N(^{4}S) number density show its highest value (3.95×10^{13} m^{-3}) at March Equinox, and its lowest value (2.48×10^{13} m^{-3}) at June solstice. The peak values of NO number density show its highest value (4.97×10^{13} m^{-3}) at June solstice, and its lowest value (2.98×10^{13} m^{-3}) at March Equinox.

3. Conclusion

In this paper, we examine the global mean structures of the ionosphere and thermosphere for geomagnetic quiet condition using a new global 3-D self-consistent model of the ionosphere and thermosphere (GCITEM-IGGCAS). GCITEM-IGGCAS model self-consistently calculates the time-dependent 3-D structure of the main parameters of the ionosphere and thermosphere for the height range from 90 to 600 km, For example, neutral number density of O_2, N_2, O, N(^{2}D), N(^{4}S), NO, He and Ar; ion number densities of O^+ ,O_2^+, N_2^+, NO^+, N^+ and electron; neutral, electron and ion temperature; neutral wind; and ionospheric electric fields. We simulates the main features of the global mean structures of the ionosphere and thermosphere using this model, and the calculated results agree well with the empirical models (MSIS and IRI). This model can also study the seasonal variation of the global mean structures of the ionosphere and thermosphere.

4. Acknowledgments

This work is supported by the Chinese Academy of Sciences (KZZD-EW-01-2), National Important Basic Research Project (2011CB811405), and National Science Foundation of China (41322030, 41321003, 41131066, 40974090).

5. References

1 D. Bilitza, "International reference ionosphere 2000." *Radio Sci.*, **36**, 2001, pp. 261–272.

2 T. J. Fuller-Rowell, D.Rees, "A three-dimensional, time-dependent, global model of the thermosphere." *J. Atmos. Sci.*, **37(11)**, 1980, pp. 2545–2567.

3 M. E. Hagan, R. G. Roble, J. Hackney, "Migrating thermospheric tides." *J. Geophys. Res.*, **106**, 2001, pp. 12,739–12,752.

4 A. Hedin, "Extension of the MSIS thermosphere model into the middle and lower atmosphere." *J. Geophys. Res.*, **96**, 1991, pp. 1159–1172.

5 L. Qian, S. C. Solomon, T. J. Kane, "Seasonal variation of thermospheric density and composition." *J. Geophys. Res.*, **114**, 2009, A01312, doi:10.1029/2008JA013643

6. Z. Ren, W. Wan, and L. Liu, "GCITEM-IGGCAS: A new global coupled ionosphere-thermosphere-electrodynamics model." *J. Atmos. Sol. Terr. Phys.*, **71(17&18)**, 2009, pp. 2064–2076.

7. A. D. Richmond, E. C. Ridley, R. G. Roble, "A thermosphere/ionosphere general circulation model with coupled electrodynamics." *Geophys. Res. Lett.*, **19(6)**, 1992, pp. 601–604.

8 Z. Zeng, A. Burns, W. Wang, et al., "Ionospheric annual asymmetry observed by the COSMIC radio occultation measurements and simulated by the TIEGCM." *J. Geophys. Res.*, **113**, 2008, A07305, doi:10.1029/2007JA012897